ED-16, pp. 64–77, Jan. 1969.
[4] M. E. Hines, "High-frequency negative-resistance circuit principles for Esaki diode applications," *Bell Syst. Tech. J.*, vol. 39, pp. 477–513, May 1960.
[5] R. W. Laton and G. I. Haddad, "The effects of doping profile on reflection-type IMPATT diode amplifiers," in *Proc. 1971 European Microwave Conf.* (Stockholm, Sweden, Aug. 1971), pp. A-5/1:1–5/1:4.
[6] W. H. Ku and E. F. Scherer, "Gain-bandwidth optimization of avalanche-diode amplifiers," *IEEE Trans. Microwave Theory Tech.* (*Special Issue on Microwave Circuit Aspects of Avalanche-Diode and Transferred Electron Devices*), vol. MTT-18, pp. 932–942, Nov. 1970.
[7] D. H. Steinbrecher and D. F. Peterson, "Small-signal model with frequency-independent elements for the avalanche region of a microwave negative-resistance diode," *IEEE Trans. Electron Devices*, vol. ED-17, pp. 883–891, Oct. 1970.
[8] D. F. Peterson and D. H. Steinbrecher, "Circuit model for characterizing the nearly linear behavior of avalanche diodes in amplifier circuits," *IEEE Trans. Microwave Theory Tech.*, vol. MTT-21, pp. 19–27, Jan. 1973.
[9] M. S. Gupta, "A small-signal and noise equivalent circuit for IMPATT diodes," *IEEE Trans. Microwave Theory Tech.* (Short Papers), vol. MTT-21, pp. 591–593, Sept. 1973.
[10] P. T. Greiling and G. I. Haddad, "Large-signal equivalent circuits of avalanche transit-time devices," *IEEE Trans. Microwave Theory Tech.* (*Special Issue on Microwave Circuit Aspects of Avalanche-Diode and Transferred Electron Devices*), vol. MTT-18, pp. 842–853, Nov. 1970.
[11] J. W. Gewartowski and J. E. Morris, "Active IMPATT diode parameters obtained by computer reduction of experimental data," *IEEE Trans. Microwave Theory Tech.*, vol. MTT-18, pp. 157–161, Mar. 1970.
[12] D. R. Decker, C. N. Dunn, and R. L. Frank, "Large-signal silicon and germanium avalanche-diode characteristics," *IEEE Trans. Microwave Theory Tech.* (*Special Issue on Microwave Circuit Aspects of Avalanche-Diode and Transferred Electron Devices*), vol. MTT-18, pp. 872–876, Nov. 1970.
[13] W. E. Schroeder and G. I. Haddad, "Nonlinear properties of IMPATT devices," *Proc. IEEE*, vol. 61, pp. 153–182, Feb. 1972.
[14] M. S. Gupta and R. J. Lomax, "A current-excited large-signal analysis of IMPATT devices and its circuit implications," *IEEE Trans. Electron Devices*, vol. ED-20, pp. 395–399, Apr. 1973.
[15] P. W. Braddock, "Experimental characterisation of avalanche-diode reflection amplifiers and locked oscillators," *Electron. Lett.*, vol. 7, pp. 42–44, Jan. 28, 1971.
[16] M. S. Gupta and R. J. Lomax, "A self-consistent large-signal analysis of a Read-type IMPATT diode oscillator," *IEEE Trans. Electron Devices*, vol. ED-18, pp. 544–550, Aug. 1971.
[17] D. M. Snider, "A one-watt CW high-efficiency X-band avalanche-diode amplifier," *IEEE Trans. Microwave Theory Tech.* (Corresp.), vol. MTT-18, pp. 963–967, Nov. 1970.
[18] Y. Takayama, "Power amplification with IMPATT diodes in stable and injection-locked modes," *IEEE Trans. Microwave Theory Tech.*, vol. MTT-20, pp. 266–272, Apr. 1972.
[19] G. B. Morgan and K. C. Siow, "Phase characteristics of microwave avalanche diode amplifiers," *Electron. Lett.*, vol. 8, pp. 280–281, June 1, 1972.
[20] H. Komizo, Y. Ito, H. Ashida, and M. Shinoda, "A 0.5-W CW IMPATT diode amplifier for high-capacity 11-GHz FM radio-relay equipment," *IEEE J. Solid-State Circuits*, vol. SC-8, pp. 14–20, Feb. 1973.
[21] W. Crowe and J. Sie, "The use of avalanche diodes in an amplifying mode to increase source output power," *Microwave J.*, vol. 12, pp. 67–69, Feb. 1969.

Analysis of Nonlinear Characteristics and Transient Response of IMPATT Amplifiers

H. J. KUNO

***Abstract*—Nonlinear characteristics, large-signal effects, and transient response of IMPATT amplifiers are analyzed leading to clear understanding of various nonlinear and large-signal phenomena which are often observed experimentally on IMPATT diodes operated as stable (linear) amplifiers or injection-locked oscillators. Effects of bandwidth on transient response of the IMPATT amplifiers as applied to phase-modulated signals and amplitude-modulated signals are investigated in detail. The relationship between the transition (switching) time and the amplifier bandwidth is derived. Capabilities and limitations of IMPATT diodes operated as stable amplifiers or injection-locked oscillators are discussed.**

Manuscript received January 24, 1973; revised April 6, 1973. This work was supported in part by the Air Force Avionics Laboratory, Air Force Systems Command, U.S. Air Force, Wright-Patterson AFB, Ohio.
The author is with Hughes Research Laboratories, Torrance, Calif. 90509.

I. Introduction

SINCE the discovery of microwave oscillation in a p-n junction diode biased into breakdown [1], [2], IMPATT (an acronym from IMPact ionization Avalanche Transit Time) devices have rapidly been developed into practical microwave power generators for system applications. In recent years, microwave power amplification with IMPATT diodes has become of great interest and importance for system applications.

Microwave power amplification can be achieved with an IMPATT diode operated as either a stable amplifier or as an injection-locked oscillator. This paper presents an analysis of nonlinear characteristics, large-signal effects, and transient response of both types of IMPATT amplifiers. The analysis leads to clear understanding of various nonlinear and large-signal phenomena which are often observed experimentally, such as constant gain–bandwidth product, gain compression or expansion, power saturation, and AM–PM conversion. The analysis also includes the effects of the amplifier bandwidth and gain saturation on transient response.

II. IMPATT Amplifier Model

Shown in Fig. 1 is a simplified equivalent circuit for a circulator-coupled IMPATT amplifier. It consists of a circulator, an impedance transformer, a tuning element, and an IMPATT diode. Although an equivalent circuit of a practical IMPATT amplifier in general may be more complex, it can be reduced to a simple form, as shown in Fig. 1, over a limited frequency range of specific interest. The IMPATT diode may be represented by a parallel combination of a negative conductance $-G_n$, a junction capacitance C_j, and an avalanche inductance L_a [3], [4]. We assume that the device is excited by a purely sinusoidal voltage waveform and that the amplitude and phase of the voltage are slowly varying functions of time in comparison with the fundamental frequency. At small-signal levels, these parameters are relatively constant. However, at large-signal levels, the diode parameters are dependent on the signal level. The nonlinear characteristics of the IMPATT diode parameters may be expressed by polynomial functions of the amplitude of the sinusoidal voltage across the diode terminals [5], [6], [12], i.e.,

$$-G_n = -g_n + \gamma V_d^2 + \sum_{n=2} a_n V_d^{2n} \tag{1}$$

$$\frac{1}{L_a} = \frac{1}{l_a} + \lambda V_d^2 + \sum_{n=2} b_n V_d^{2n} \tag{2}$$

$$C_j = \text{constant} \tag{3}$$

where $-g_n$ and l_a are small-signal parameters; γ, λ, and A_n, b_n are constants; and V_d is the amplitude of the sinusoidal voltage across the diode terminals, as shown in Fig. 1. In the region of practical IMPATT amplifier operation where the amplitude of the sinusoidal voltage is much smaller than the dc bias voltage the higher order terms in (1) and (2) may be neglected. Then (1) and (2) reduce to Van der Pol-type nonlinearities [7]. The equivalent load admittance seen from the diode terminals is represented by

$$Y_L = G_L - j(1/\omega L_{\text{ext}}). \tag{4}$$

Since the imaginary component of the diode is capacitive at a normal operation frequency, an inductive load is required for tuning. The equivalent voltage and current components of the incident and the reflected waves are represented by V_i, i_i, V_r, and i_r, where the subscripts i and r, respectively, refer to the incident and reflected waves. The incident and reflected waves are separated into the input and output signals by the circulator. The net current into the diode i_d and voltage across the diode terminals V_d are given by

$$V_d = V_i + V_r \tag{5}$$

$$i_d = i_i - i_r = G_L(2V_i - V_d). \tag{6}$$

In the equivalent circuit of Fig. 1, i_d and V_d are governed by a nonlinear integral–differential equation given by

$$i_d = \int_{-\infty}^{t} \left(\frac{1}{L_{\text{ext}}} + \frac{1}{L_a}\right) V_d \, dt - G_n V_d + C_j \left(\frac{dV_d}{dt}\right). \tag{7}$$

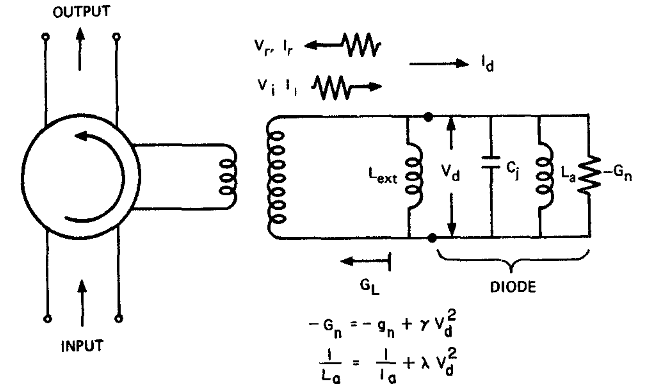

Fig. 1. An equivalent circuit of a circulator-coupled IMPATT amplifier.

Substituting (1)–(6) into (7), we get

$$\left(\frac{2G_L}{C_j}\right)\frac{dV_i}{dt} = \frac{d^2V_d}{dt^2} - \left(\frac{1}{C_j}\right)(g_n - G_L - 3\gamma V_d^2)\left(\frac{dV_d}{dt}\right) + \left(\omega_0^2 - \frac{\lambda}{C_j} V_d^2\right) V_d \tag{8}$$

where

$$\omega_0^2 = \left(\frac{1}{L_{\text{ext}}} + \frac{1}{l_a}\right)\frac{1}{C_j}. \tag{9}$$

Let us assume that the circuit Q is relatively high and that V_i, V_r, and V_d are given by the form:

$$V_i = V_0 A_i(t) \sin [\omega t + \phi_i(t)] \tag{10}$$

$$V_r = V_0 A_r(t) \sin [\omega t + \phi_t(t)] \tag{11}$$

$$V_d = V_0 A_d(t) \sin [\omega t + \phi_d(t)] \tag{12}$$

where V_0 is an arbitrary nonzero constant and ω is the angular frequency of the input signal. $A(t)$ and $\phi(t)$ are, respectively, amplitude- and phase-modulation functions. We assume that both $A(t)$ and $\phi(t)$ are slowly varying functions of time in comparison with the carrier frequency, i.e.,

$$\frac{dA}{dt} \ll \omega A \quad \text{and} \quad \frac{d\phi}{dt} \ll \omega \tag{13}$$

and that the carrier frequency is close to the resonant frequency, i.e.,

$$\omega \simeq \omega_0. \tag{14}$$

Note that since V_i, V_r, and V_d are related by (6), we also have

$$\begin{cases} A_r = [A_i^2 + A_d^2 - 2A_iA_d \cos (\phi_i - \phi_i)]^{1/2} & (15) \\ \phi_r = \tan^{-1}\left[\dfrac{A_d \sin \phi_d - A_i \sin \phi_i}{A_d \cos \phi_d - A_i \cos \phi_i}\right]. & (16) \end{cases}$$

Substituting (10)–(12) into (8), making use of conditions given by (13) and (14), and retaining only terms involving the fundamental frequency, e.g., $\sin^3 \psi \simeq 3/4 \sin \psi$, we can derive a set of coupled differential equations that govern the amplitude and phase by the following method.

Multiply the resulting equation by $\cos (\omega t + \phi_d)$ and integrate over a period. Similarly, multiply the equation by sin $(\omega t+\phi_d)$ and integrate over a period [8]. After simplifying the resulting equations by the relationships given by (13) and (14), we obtain [15]

$$\left(\frac{2}{\omega_0}\right)\frac{dA_d}{dt} + (A_d^2 - \epsilon)A_d = \eta A_i \cos(\phi_i - \phi_d) \tag{17}$$

$$\left(\frac{2}{\omega_0}\right)A_d\frac{d\phi_d}{dt} + (\beta A_d^2 + \delta)A_d = \eta A_i \sin(\phi_i - \phi_d) \tag{18}$$

where

$$\epsilon = \frac{g_n - G_L}{\omega_0 C_j}$$

$$V_0^2 = \frac{4}{9}\left(\frac{\omega_0 C_j}{\gamma}\right)$$

$$\beta = \frac{3\lambda V_0^2}{4\omega\omega_0 C_j} \simeq \frac{\lambda}{3\omega_0\gamma}$$

$$\delta = \frac{\omega}{\omega_0} - \frac{\omega_0}{\omega} \simeq \frac{2}{\omega_0}(\omega - \omega_0)$$

$$\eta = \frac{2G_L}{\omega_0 C_j}$$

$$\omega_0^2 = \left(\frac{1}{L_{\text{ext}}} + \frac{1}{l_a}\right)\frac{1}{C_j}\cdot \tag{19}$$

From (17) and (18), A_d and ϕ_d are to be solved for a given set of input signal amplitude function $A_i(t)$ and phase function $\phi_i(t)$. Note that A_d and ϕ_d do not refer to the output signal. The output amplitude and phase functions $A_r(t)$ and $\phi_r(t)$, respectively, must be obtained from the relationships given by (15) and (16). In the following sections, steady-state behaviors and transient response of IMPATT oscillators and amplifiers under various conditions are analyzed.

III. Free-Running Oscillation

Let us first consider a free-running condition, i.e., $A_i=0$ in (17) and (18). In this case, we have

$$\left(\frac{2}{\omega_0}\right)\frac{dA_d}{dt} = -(A_d^2 - \epsilon)A_d \tag{20}$$

$$\left(\frac{2}{\omega_0}\right)\frac{d\phi_d}{dt} = -(\beta A_d^2 + \delta). \tag{21}$$

Note that ϵ may be either positive or negative depending on loading conditions. If $\epsilon<0$, i.e., $G_L>g_n$, dA_d/dt becomes negative for any positive values of A_d. This means that the oscillation is decaying. And only when $A_d=0$, dA_d/dt becomes zero. Thus, when $G_L>g_n$, the IMPATT diode is stable and no free-running oscillation exists and no output power is generated.

If $\epsilon>0$, i.e., $G_L<g_n$, and $A_d^2<\epsilon$, then dA_d/dt is positive indicating that the oscillation is growing. If $A_d^2>\epsilon$, then dA_d/dt becomes negative indicating that the amplitude of oscillation is decreasing. Steady oscillation can be found when $A_d^2=\epsilon$. Although when $A_d^2=0$, dA_d/dt also becomes zero, any small disturbance such as noise can trigger growing oscillation. Thus, when $\epsilon>0$, the IMPATT diode is unstable and the amplitude of the steady-state oscillation is determined by

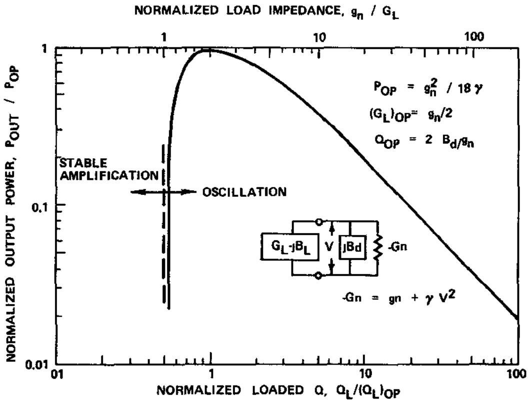

Fig. 2. Effect of load on output power of an IMPATT oscillator.

$$A_r^2 = A_d^2 = \epsilon. \tag{22}$$

And the output power delivered to the load G_L is given by

$$P_{\text{out}} = (1/2)V_0^2A_r^2G_L = V_0^2\epsilon G_L$$

$$= (2/9)\left(\frac{g_n - G_L}{\gamma}\right)G_L \tag{23}$$

and the free-running frequency given by

$$\omega_{\text{osc}} = \omega_0\left(1 - \frac{\beta\epsilon}{2}\right)$$

$$= \omega_0 - \left(\frac{\lambda}{6\gamma}\right)\left(\frac{g_n - G_L}{\omega_0 C_j}\right). \tag{24}$$

From (23) we find that the maximum output power can be achieved when $G_L=g_n/2$ and the maximum output power is given by

$$P_{\text{op}} = \frac{1}{18}\left(\frac{g_n^2}{\gamma}\right). \tag{25}$$

In Fig. 2, variation of output power as a function of load as given by (23) is plotted.

IV. Stable Amplifier

For steady-state condition, i.e.,

$$\frac{dA_d}{dt} = \frac{d\phi_d}{dt} = 0$$

(17) and (18) become

$$(A_d^2 - \epsilon)A_d = \eta A_i \cos(\phi_i - \phi_d) \tag{26}$$

$$(\beta A_d^2 + \delta)A_d = \eta A_i \sin(\phi_i - \phi_d). \tag{27}$$

It was shown that when $\epsilon<0$, i.e., $G_L>g_n$, the IMPATT diode is stable. For a small-signal condition, i.e., $A_d^2\ll\epsilon$, we get

$$-\epsilon(A_d/A_i) = \eta\cos(\phi_i - \phi_d) \tag{28}$$

$$\delta(A_d/A_i) = \eta\sin(\phi_i - \phi_d). \tag{29}$$

At the center frequency ω_0 we get $\phi_i-\phi_d=0$, and the power gain is given by

$$\left(\frac{A_r}{A_i}\right)^2=\left(\frac{A_d}{A_i}-1\right)^2=\left(-\frac{\eta}{\epsilon}-1\right)^2=\left(\frac{G_L+g_n}{G_L-g_n}\right)^2 \quad (30)$$

as one expects from a transmission-line reflection equation.

From (15), (16), and (28), we find that the gain at a given frequency may be given by

$$G(\omega)=\left(\frac{A_r}{A_i}\right)^2=1+\left(\frac{A_d}{A_i}\right)^2-2\left(\frac{A_d}{A_i}\right)\cos(\phi_i-\phi_d)$$
$$=1+\left(\frac{\eta}{\epsilon}+2\right)\left(\frac{\eta}{\epsilon}\right)\cos^2(\phi_i-\phi_d).$$

Noting that, from (30),

$$-\frac{\eta}{\epsilon}=\sqrt{G_0}+1$$

we get

$$\frac{G(\omega)-1}{G_0-1}=\cos^2(\phi_i-\phi_d).$$

If we define the amplifier bandwidth $2\Delta\omega$ in such a way that, at $\omega_\pm=\omega_0\pm\Delta\omega$, gain becomes

$$\frac{G_\pm-1}{G_0-1}=\frac{1}{2} \quad (31)$$

where $G_\pm=G(\omega_0\pm\Delta\omega)$, $G_0=G(\omega_0)$, ω_0 equals midband frequency, then, from (28) and (29), we get

$$\left(\frac{2\Delta\omega}{\omega_0}\right)(\sqrt{G_0}+1)=\eta=\text{constant}. \quad (32)$$

For $G_0\gg 1$ as in most amplifiers this reduces to the conventional definition of normalized gain–bandwidth product, i.e.,

$$\left(\frac{2\Delta\omega}{\omega_0}\right)\sqrt{G_0}\cong\eta \quad (33)$$

where $2\Delta\omega$ is defined by $G(\omega_0\pm\Delta\omega)=G(\omega_0)/2$. For a range of practical interest where $G_0\gg 1$, G_L does not vary appreciably for a large variation of gain. Thus the normalized gain–bandwidth product given by (32) remains relatively constant for a wide range of gain variation. For this reason the gain–bandwidth product is used as a measure of the amplifier quality.

V. Injection-Locked Oscillator

In Section III it was shown that, when $\epsilon>0$, i.e., $G_L<g_n$, the IMPATT diode becomes unstable and results in oscillation at a frequency given by

$$\omega_{osc}=\omega_0\left(1-\frac{\beta\epsilon}{2}\right)=\omega_0-\left(\frac{\lambda}{6\gamma}\right)\left(\frac{g_n-G_L}{\omega_0C_j}\right) \quad (34)$$

and the amplitude of oscillation given by

$$A_d=\sqrt{\epsilon}=\frac{g_n-G_L}{\omega_0C_j}. \quad (35)$$

The oscillating IMPATT diode can also be used for amplification of microwaves by means of injection locking. For a given A_i in (28) and (27), a real steady-state solution for A_d can be found only in the region where

$$-\frac{\pi}{2}\le(\phi_i-\phi_d)\le\frac{\pi}{2}.$$

Physically, this means that the oscillation cannot be locked to the input signal outside of this region. For a small input signal level, i.e., $A_i^2\ll A_d^2$, we get $A_d^2\simeq\epsilon$. Then, since $\sin(\phi_i-\phi_d)\lesssim 1$, at the edge of the locking band, viz., $\omega_\pm=\omega_{osc}\pm\Delta\omega$, we get

$$(\beta\epsilon+\delta)\left(\frac{A_d}{A_i}\right)=\frac{2\Delta\omega}{\omega_0}(\sqrt{G}+1)=\eta \quad (36)$$

and

$$\phi_i-\phi_d=\pm\frac{\pi}{2}.$$

Note that η is constant for a given loading condition. Thus the normalized locking gain–bandwidth product given by (36), which is a measurement of the injection-locked oscillator, is constant for a given loading condition.

Thus, for both a stable amplifier and an injection-locked oscillator, the normalized gain–bandwidth product is equal to $\eta=(2G_L/\omega_0 C_j)$. Comparing (32) and (36), and noting that, for a given IMPATT diode, a stable amplifier requires a larger value of G_L than an oscillator, we can see that it is easier to obtain a larger gain–bandwidth product with a stable IMPATT amplifier than with an injection-locked oscillator. It should be noted that any parasitic capacitance such as a package capacitance placed in parallel with C_j will in effect reduce the gain–bandwidth product of the amplifier.

VI. Large-Signal Effects

In order to analyze the large-signal effects, (26) and (27) must be solved. The coupled nonlinear differential equations can be solved numerically to evaluate output versus input power characteristics of an IMPATT diode. Shown in Fig. 3 are the output versus input power characteristics of IMPATT amplifiers and those of injection-locked oscillators numerically calculated from (26) and (27) together with (15) and (16) at center frequencies, i.e., $\omega=\omega_0$ for stable amplifiers and $\omega=\omega_{osc}$ for injection-locked oscillators. The loading conditions determine the small-signal gain and bandwidth. The output power and the input power are normalized to the optimally loaded oscillation power given by (25). An injection-locked oscillator yields high output power with a higher

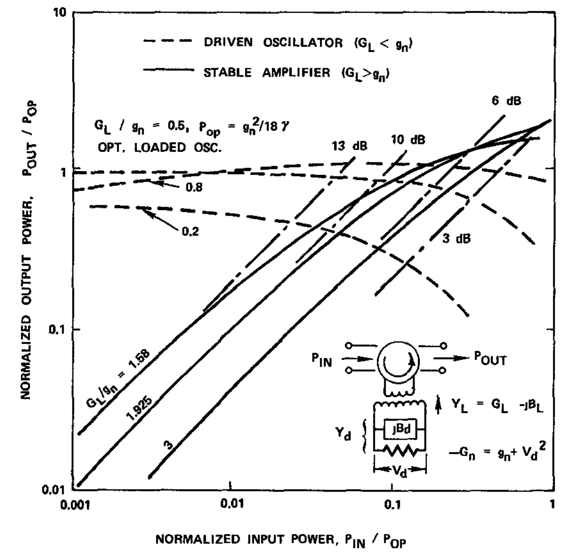

Fig. 3. Power saturation characteristics of IMPATT amplifiers.

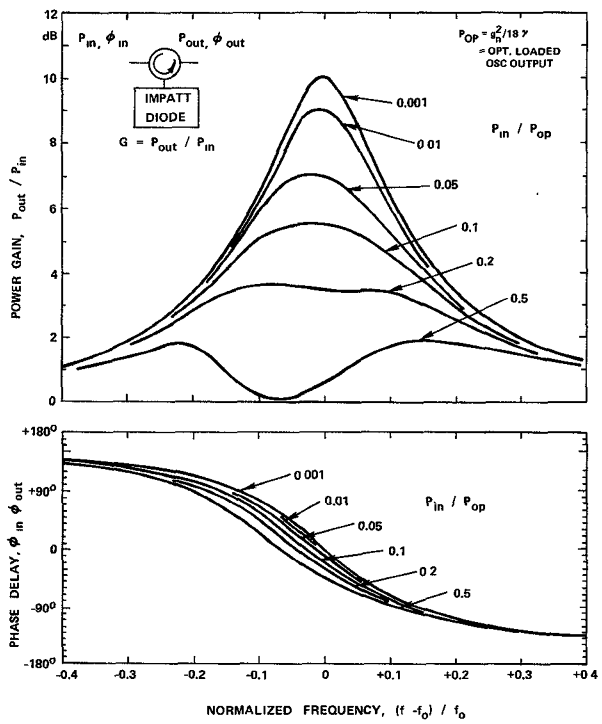

Fig. 4. Effects of input signal level on gain and bandwidth characteristics of stable IMPATT amplifier.

gain (with a narrow bandwidth), while a stable amplifier yields high output with a relatively low gain (with a broader bandwidth).

From (26) and (27) together with (15) and (16), nonlinear characteristics of IMPATT amplifiers under various conditions can be calculated. Fig. 4 shows calculated effects of the input signal level on the bandpass and phase characteristics of a stable IMPATT amplifier tuned to a small-signal gain of 10 dB. The input and output power levels are normalized to the optimally loaded oscillator power $P_{op} = g_n^2/18\ \gamma$ and the frequency is normalized to $f_0 = \omega_0/2\pi$. It can be seen that as the input signal level increases the gain decreases, the bandwidth increases, and the center frequency shifts to the lower side.

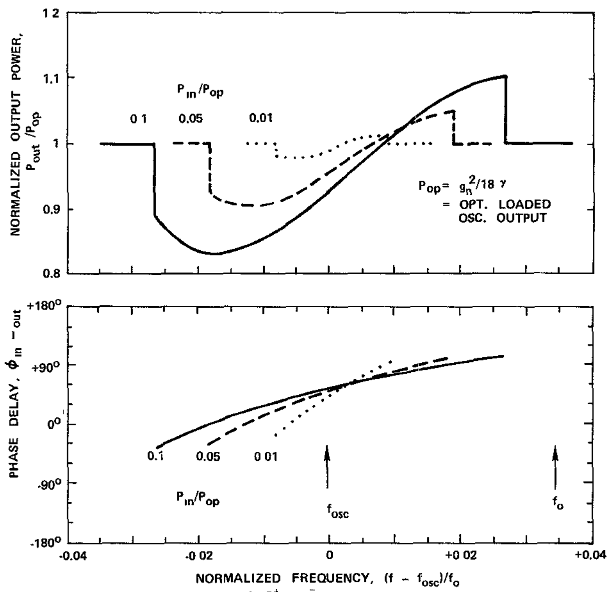

Fig. 5. Effects of input signal level on injection-locking characteristics of IMPATT oscillator.

The lowering of the center frequency may result in gain expansion with increasing input signal level at the lower half of the amplifier passband under certain conditions such as a high-gain narrow-band amplifier. Experimental observation of this phenomenon has been reported in many papers. It is also interesting to note the pronounced decrease in gain near the center of the amplifier band at high input signal levels, i.e., $P_{in} > 0.2\ P_{op}$. This nonlinear effect has also been observed experimentally [9].

Shown in Fig. 5 are locking characteristics of an IMPATT diode similarly calculated. The locking characteristics of the injection-locked IMPATT oscillator were found not to be symmetrical about the frequency of free-running oscillation This is contrary to the results of earlier analyses [10]–[12] on injection-locking phenomena, but it is in agreement with the experimental results [9], [13], [18] and also with recent analyses of X-band IMPATT diodes [18]–[20].

In Figs. 6 and 7 the large-signal effects are shown differently. Variations of phase shift and power gain calculated for a stable IMPATT amplifier tuned to 10-dB small-signal gain are plotted as a function of input signal power level. At small-signal levels (linear amplification) both power gain and phase shift remain constant. At large-signal levels phase and gain will change due to the nonlinear characteristics of the diode parameter. This results in various nonlinear effects such as AM–PM conversion and intermodulation. In an injection-locked oscillator, both phase shift and output power vary with signal level even at very low input power levels except at $\omega = \omega_{osc}$ where the output power and phase shift remain fairly constant at low signal levels.

VII. Transient Response

In addition to the steady-state characteristics, the transient response of an IMPATT amplifier that determines data-rate capability is also of greater importance. The transient response of an IMPATT amplifier can be analyzed by solving for output and phase responses $A_r(t)$ and $\phi_r(t)$ to given input amplitude and phase waveforms $A_i(t)$ and $\phi_i(t)$ from (15)–(18). In this section, transient responses of IMPATT amplifiers

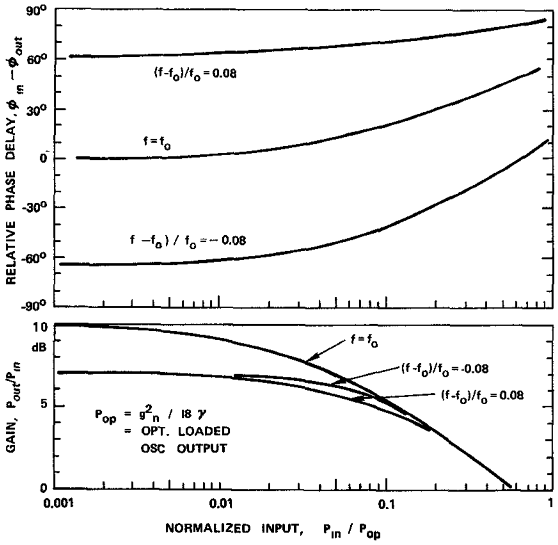

Fig. 6. Large-signal effects on gain and phase delay of a stable IMPATT amplifier.

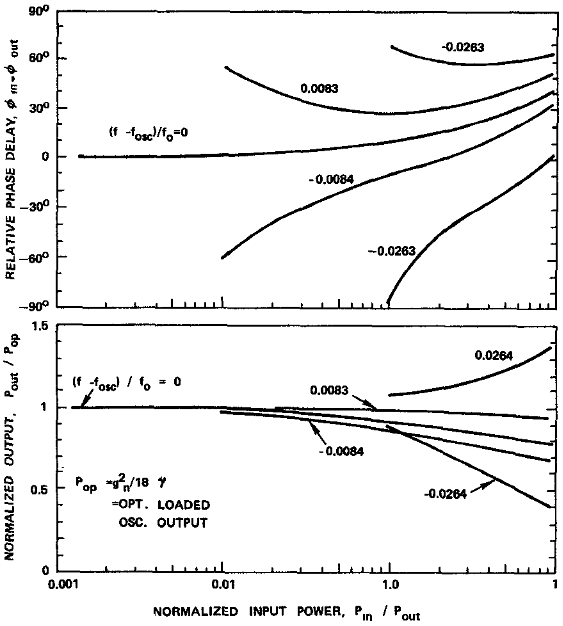

Fig. 7. Large-signal effects on output power and phase delay of an injection-locked IMPATT oscillator.

to both phase-modulated signals and amplitude-modulated signals, which are two major areas of IMPATT amplifier applications, are analyzed.

Power amplification of phase-modulated signals can be accomplished either with a stable IMPATT amplifier or with an injection-locked IMPATT oscillator. Note that the transient responses of both a stable amplifier and an injection-locked oscillator are governed by the same set of equations. For biphase modulation, $\phi_i(t)$ changes either from 0° to 180° or from 180° to 0°. Examination of (18) shows that, in order to achieve symmetrical phase transitions, we must have [15]

$$\beta A_d^2 + \delta = 0. \tag{37}$$

This means that the signal frequency should be set at a frequency given by

$$\omega_s = \omega_0\left(1 - \frac{\beta A_d^2}{2\omega_0}\right). \tag{38}$$

This is the midband frequency for a stable amplifier and the free-running oscillation frequency for an injection-locked oscillator. This result is contrary to the results of earlier works [10], [11], [14] which have shown that the signal frequency should be set away from the center frequency to achieve optimum transition time. The conclusions of the earlier works are based on simplified analyses carried out for cases where the input signal changes phase instantaneously (step function) with no change in amplitude. In a real system, however, the input signal does have a finite transition time [15], [16]. Thus, in this paper, we analyze the transient response of an IMPATT amplifier to an input signal with a finite transition time at a center frequency given by (38).

In solving (17) and (18) it is convenient to normalize time t and bandwidth $2\Delta f$ to the input signal transition time T_s (measured from 10 to 90 percent of total transition), i.e.,

$$T = t/T_s$$
$$B = 2\Delta f T_s.$$

We have numerically solved (17) and (18) for $A_d(t)$ and $\phi_d(t)$, then for $A_r(t)$ and $\phi_r(t)$ under various conditions of gain and bandwidth. Detailed analysis has shown the transient response is most sensitive to the amplifier bandwidth and that it is not very sensitive to the amplifier gain. Figs. 8 and 9 are effects of bandwidth on the amplitude and phase transient response of a stable IMPATT amplifier and an injection-locked oscillator, respectively. The power gain was set at a typical value of 13 dB.

In Figs. 8 and 9 input power and output power are normalized to their steady-state values. It can be seen that bandwidth required to amplify phase-modulated signals with transition time T_s without increase in output phase transition time is

$$2\Delta f \geq 1/T_s$$

for both an injection-locked IMPATT oscillator and a stable IMPATT amplifier. As the bandwidth decreases, the output-power transition time increases. Comparison of Figs. 8 and 9 shows that, for the same bandwidth, faster output phase transition time can be obtained with a stable amplifier than with an injection-locked oscillator. However, the phase transition in a stable amplifier is accompanied by a significant amount of amplitude modulation which increases with decreasing bandwidth.

In Figs. 8 and 9 it is assumed that the input signal has a constant amplitude during the phase transition time. In a real phase modulator, however, the phase modulation is accompanied by amplitude modulation [16]. The amplitude modulation is caused by increased insertion loss in transition state as shown in Fig. 10 where phase shift and insertion loss of a typical p-i-n diode phase modulator are plotted as a function of bias. Shown in Figs. 11 and 12 are effects of the amplitude modulation accompanying the phase-modulated input signal on the output phase and amplitude transient responses of stable IMPATT amplifiers and injection-locked oscillators. Note that the amplitude modulation of the input signal results in hesitation of the output phase transition. Suppression of the output amplitude modulation can be seen in the injection-locked oscillator. It is interesting to compare the

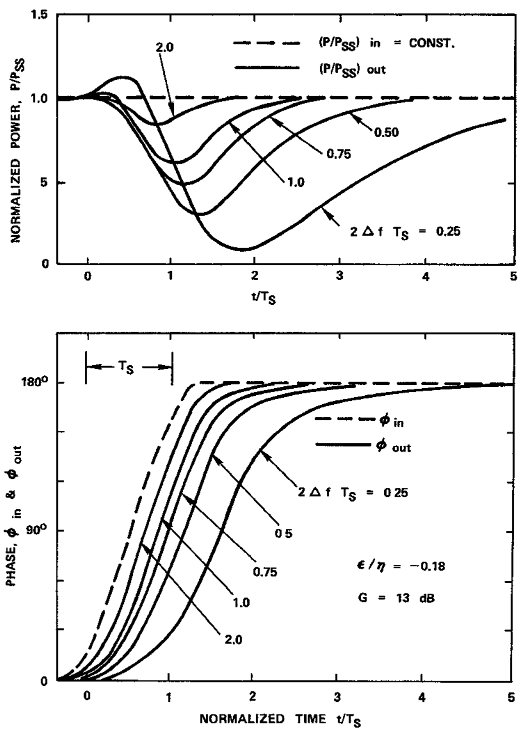

Fig. 8. Effect of bandwidth on transient response of a stable IMPATT amplifier to a phase-modulated signal.

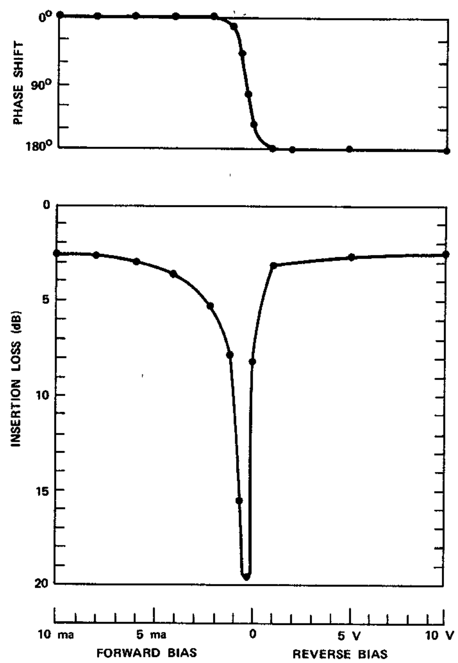

Fig. 10. Variations of insertion loss and phase shift of a p-i-n diode biphase modulator as a function of bias.

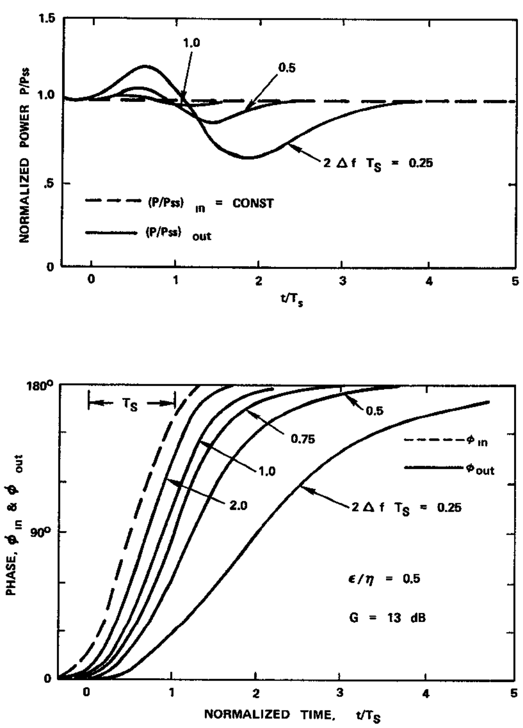

Fig. 9. Effect of bandwidth on transient response of an injection-locked IMPATT oscillator to a phase-modulated signal.

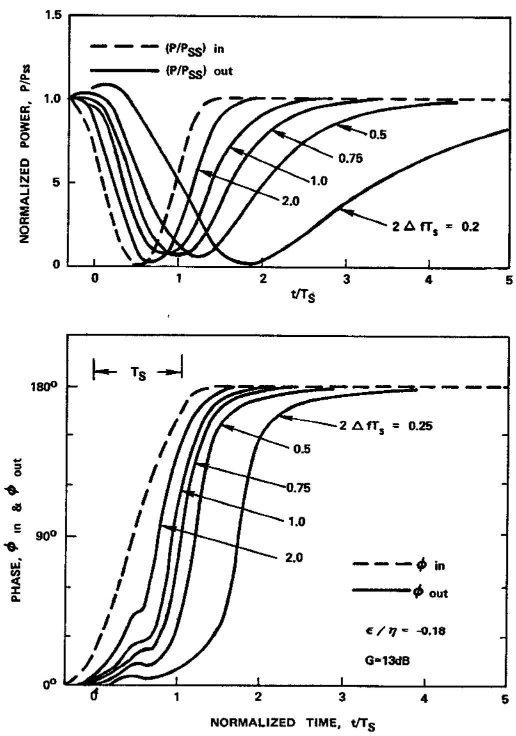

Fig. 11. Transient response of a stable IMPATT amplifier when phase-modulated input signal is accompanied by amplitude modulation.

calculated waveforms shown in Fig. 12 with those shown in Fig. 13, which were measured on an injection-locked IMPATT oscillator for various locking bandwidths. Remarkable agreement can be seen, including the initial hesitation in phase transition.

Fig. 14 shows effects of gain saturation on the transient response. It can be see that, for a given device operated as a stable amplifier, gain saturation results in faster phase transition due to the bandwidth broadening.

Shown in Fig. 15 are effects of bandwidth on transient

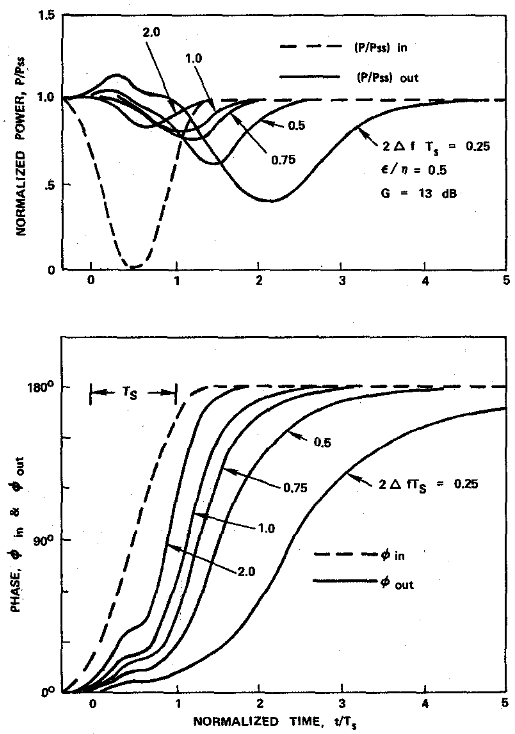

Fig. 12. Transient response of an injection-locked oscillator when phase-modulated input signal is accompanied by amplitude modulation.

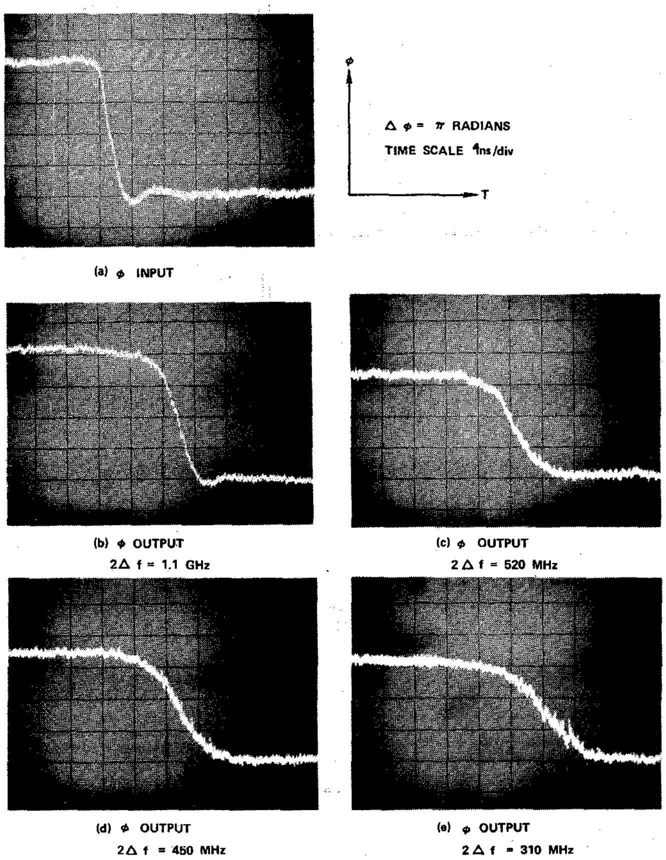

Fig. 13. Measured transient response of an injection-locked IMPATT oscillator for various bandwidths.

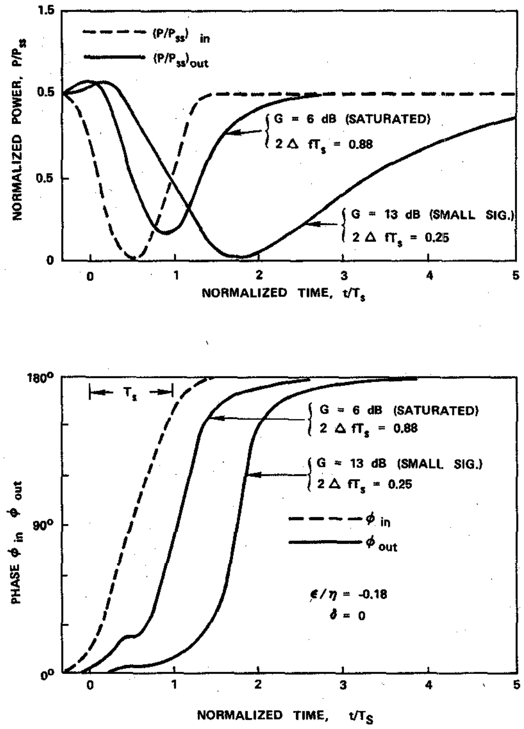

Fig. 14. Effects of gain saturation on transient response of an IMPATT amplifier.

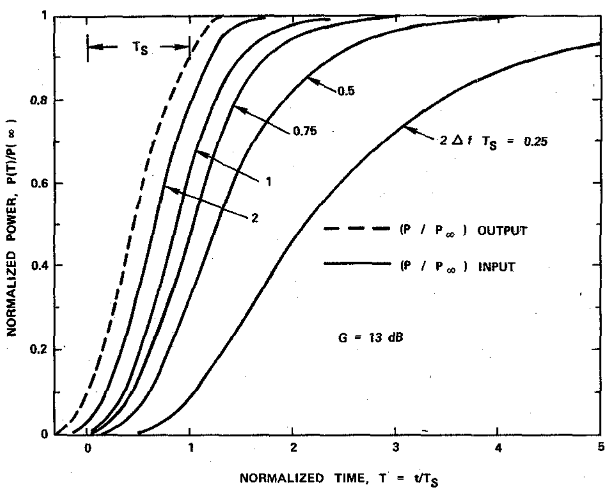

Fig. 15. Effects of bandwidth on transient response of an IMPATT amplifier to an amplitude-modulated signal.

response of a stable IMPATT amplifier to amplitude modulated signals. The small-signal gain is set at 13 dB. The amplifier transient response is not sensitive to gain. However, the transient response is affected by the input signal level, as shown in Fig. 16.

For the same small-signal bandwidth, faster output transition can be achieved with a saturated amplifier than with an unsaturated linear amplifier. This is due to the fact that the bandwidth increases as gain compression occurs due to the large-signal effect.

VIII. Conclusions

It has been shown that an IMPATT diode can be operated as an injection-locked oscillator as well as a stable amplifier for

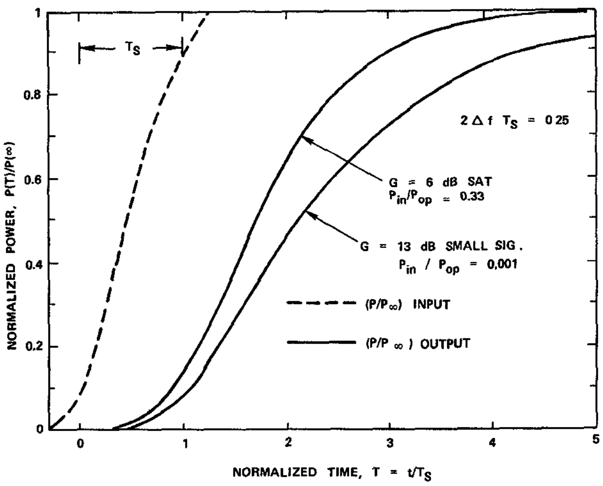

Fig. 16. Effects of gain saturation on transient response of an IMPATT amplifier to an amplitude-modulated signal.

microwave power amplification. The preceding analysis shows that, for a given IMPATT diode, a higher output power can be achieved with an injection-locked oscillator with high-gain (>10 dB) narrow-bandwidth characteristics, while a stable amplifier yields a linear gain at low power levels and high output power with relatively low gain (<10 dB) and broad bandwidth. The stable IMPATT amplifier can generate as much added power as an optimally loaded oscillator when driven to low saturated gain (~3 dB). For a given diode, a larger gain–bandwidth product can be achieved with a stable amplifier than with an injection-locked oscillator. The transient-response analysis carried out in this paper has shown that the switching time T_s and amplifier bandwidth $2\Delta f$ are related by $2\Delta f \cong 1/T_s$. Since bandwidths greater than 2 GHz can be achieved with IMPATT amplifiers, IMPATT diodes can be used effectively for power amplification in high data-rate communication systems with modulation rates beyond 1 Gbit/s with transition time less than 0.5 ns [16]. The analysis has also shown that to achieve the maximum modulation rate, the signal frequency should be set at a midband frequency for a stable amplifier or at a free-running oscillation frequency for an injection-locked oscillator.

Comparison of various nonlinear characteristics and large-signal phenomena described by the preceding analysis with experimental results shows remarkable agreement [13], [17]. The analysis can be extended readily to many cases other than those described in this paper, such as sinusoidal modulation, quadriphase modulated signals, and multiple-stage amplifiers.

References

[1] R. L. Johnston, B. C. Loach, Jr., and G. B. Cohen, "A silicon diode microwave oscillator," *Bell Syst. Tech. J.*, vol. 44, pp. 369–372, Feb. 1965.

[2] W. T. Read, "A proposed high-frequency negative resistance diode," *Bell Syst. Tech. J.*, vol. 37, pp. 401–446, Mar. 1958.

[3] T. Misawa, "Negative resistance in *p-n* junctions under avalanche breakdown conditions," *IEEE Trans. Electron Devices* (*Special Issue on Semiconductor Bulk-Effect and Transit-Time Devices*), vol. ED-13, pp. 137–151, Jan. 1966.

[4] M. Gilden and M. E. Hines, "Electronic tuning effects in the Read microwave avalanche diode," *IEEE Trans. Electron Devices* (*Special Issue on Semiconductor Bulk-Effect and Transit-Time Devices*), vol. ED-13, pp. 169–175, Jan. 1966.

[5] N. B. Kramer, "Characterization and modeling of IMPATT oscillators," *IEEE Trans. Electron Devices*, vol. ED-15, pp. 838–846, Nov. 1968.

[6] J. W. Gewartowski and J. E. Morris, "Active IMPATT diode parameters obtained by computer reduction of experimental data," *IEEE Trans. Microwave Theory Tech.*, vol. MTT-18, pp. 157–161, Mar. 1970.

[7] B. Van der Pol, "Forced oscillations in a circuit with nonlinear resistance (reception with reactive triode)," *Phil. Mag.*, ser. 7, vol. 3, pp. 65–80, Jan. 1927.

[8] N. N. Bogliubov and Y. A. Mitropolsky, *Asymptotic Methods in the Theory of Nonlinear Oscillations.* New York: Gordon and Breach, 1961.

[9] E. F. Scherer, "Large-signal operation of avalanche-diode amplifiers," *IEEE Trans. Microwave Theory Tech.* (*Special Issue on Microwave Circuit Aspects of Avalanche-Diode and Transferred Electron Devices*), vol. MTT-18, pp. 922–932, Nov. 1970.

[10] R. Adler, "A study of locking phenomena in oscillators," *Proc. IRE*, vol. 34, pp. 351–357, June 1946.

[11] R. C. MacKey, "Injection locking of klystron oscillators," *IRE Trans. Microwave Theory Tech.*, vol. MTT-10, pp. 228–235, July 1962.

[12] M. E. Hines, "Negative-resistance diode power amplification," *IEEE Trans. Electron Devices*, vol. ED-17, pp. 1–8, Jan. 1970.

[13] H. J. Kuno and D. L. English, "Nonlinear and large signal characteristics of millimeter-wave IMPATT amplifiers," *IEEE Trans. Microwave Theory Tech.*, this issue, pp. 703–706.

[14] Y. Fukatsu, M. Akaike, and H. Kato, "Amplification of high speed PCM phase-shift keyed millimeter-wave signals through an injection locked IMPATT oscillator," presented at the 1971 IEEE Int. Solid-State Circuits Conf., Philadelphia, Pa., Feb. 1971.

[15] H. J. Kuno, L. S. Bowman, and D. L. English, "Millimeter-wave silicon IMPATT power amplifiers for phase-modulated signals," presented at the 1971 IEEE Int. Solid-State Circuits Conf., Philadelphia, Pa., Feb. 1971.

[16] H. J. Kuno, D. L. English, and P. H. Pusateri, "Millimeter-wave solid state exciter/modulator-amplifier module for gigabit data-rate," presented at the 1972 IEEE Int. Microwave Symp., Chicago, Ill., May 1972.

[17] H. J. Kuno, D. L. English, and R. S. Ying, "High power millimeter-wave IMPATT amplifiers," presented at the 1973 IEEE Int. Solid-State Circuits Conf., Philadelphia, Pa., 1973.

[18] Y. Takayama, "Power amplification with IMPATT diodes in stable and injection-locked modes," *IEEE Trans. Microwave Theory Tech.*, vol. MTT-20, pp. 266–272, Apr. 1972.

[19] ——, "Dynamic behavior of nonlinear power amplifiers in stable and injection-locked modes," *IEEE Trans. Microwave Theory Tech.*, vol. MTT-20, pp. 591–595, Sept. 1972.

[20] L. Gustafsson, G. H. B. Hansson, and K. I. Lundstrom, "On the use of describing functions in the study of nonlinear active circuits," *IEEE Trans. Microwave Theory Tech.*, vol. MTT-20, pp. 402–409, June 1972.